Multiferroicity in the spin-1/2 quantum matter of $LiCu_2O_2$

A. Rusydi,[1,a)] I. Mahns,[1] S. Müller,[1] M. Rübhausen,[1] S. Park,[2] Y. J. Choi,[2] C. L. Zhang,[2] S.-W. Cheong,[2] S. Smadici,[3] P. Abbamonte,[3] M. v. Zimmermann,[4] and G. A. Sawatzky[5]

[1]*Institut für Angewandte Physik, Universität Hamburg, Jungiusstraβe 11, D-20355 Hamburg, Germany*
[2]*Department of Physics and Astronomy, Rutgers University, Piscataway, New Jersey 08854, USA*
[3]*Physics Department and Frederick Seitz Materials Research Laboratory, University of Illinois, Urbana, Illinois 6180, USA*
[4]*Hamburger Synchrotronstrahlungslabor (HASYLAB) at Deutsches Elektronen-Synchrotron (DESY), Notkestraße 85, 22603 Hamburg, Germany*
[5]*Department of Physics and Astronomy, University of British Columbia, Vancouver, British Columbia V6T-1Z1, Canada*

(Received 2 July 2007; accepted 2 September 2007; published online 2 July 2008)

Multiferroicity in $LiCu_2O_2$ single crystals is studied using resonant soft x-ray magnetic scattering, hard x-ray diffraction, heat capacity, magnetic susceptibility, and electrical polarization. Two magnetic transitions are found at 24.6 K (T_1) and 23.2 K (T_2). Our data are consistent with a sinusoidal spin structure at $T_2<T<T_1$ and with a helicoidal spin structure at $T<T_2$, giving rise to ferroelectricity. Surprisingly, above T_2, the correlation lengths of the spin structures increase as the temperature increases with dramatic changes of ~42% occurring along the c axis. © *2008 American Institute of Physics*. [DOI: 10.1063/1.2787973]

Low-dimensional spin $(S)=1/2$ copper-oxides have posed some of the most challenging problems in solid state physics. The interplay between frustration and quantum spin fluctuations results in a rich phase diagram and unusual magnetic properties. In a model with quantum $S=1/2$ chains and competing nearest-neighbor interactions J_1 and next-nearest-neighbor interactions J_2, one expects, depending on J_1/J_2, a gapless collinear phase, a gapped disordered dimer liquid phase, or a quasi long-range ordered helicoidal spin structure.[1]

$LiCu_2O_2$ consists of an equal number of Cu^{1+} and Cu^{2+} (Fig. 1(a)). The magnetic Cu^{2+} ions carry $S=1/2$ and are located at the center of edge-sharing CuO_4 plaquettes and form two frustrated quasi-one-dimensional chains along the b axis. These chains are separated by Li^{1+} to form double layers parallel to the ab plane, which are separated by Cu^{1+} sites. The Cu–O–Cu angle is ~94°. As a result, J_2 is weaker than J_1. The strength of the interaction between chains (J_{DC}) is not clear; however, J_1 is ferromagnetic and J_2 is antiferromagnetic.[2] This leads to frustration and favors helimagnetism.[1] A similar scenario was recently proposed for an isostructural $NaCu_2O_2$.[3]

$LiCu_2O_2$ exhibits striking properties such as the presence of a spin-singlet liquid state,[4] incommensurate (IC) magnetic order,[5] as well as ferroelectricity.[6] However, there is no clear understanding connecting all these properties. One problem is the intrinsic chemical disorder. Electron-spin resonance[4] has shown the presence of a spin-singlet state with a spin gap of about 6 meV at 23 K. Specific heat[4] and nuclear magnetic resonance[7] show phase transitions at 24.2, 22.5, and 9 K. Recent neutron diffraction[5] found one transition to IC magnetic superstructure below 22 K with a propagation vector $[(2n+1)/2,k+\delta,l]$, where n, k, and l are integers and δ ~0.174. It is concluded that the magnetic superstructure is a helical in the ab plane. This is inconsistent with the observation of ferroelectricity with an electric polarization along the c direction below ~23 K.[6] In an attempt to understand the coupling between lattice, charge, and spin degrees we have studied $LiCu_2O_2$ single crystal using polarization dependent resonant soft x-ray magnetic scattering (RSXMS), hard x-ray diffraction (HXD), heat capacity, magnetic susceptibility, and electrical polarization, from the same sample.

The $LiCu_2O_2$ single crystal was grown by the self-flux method.[6] The HXD was done at the beamline BW5 of HASYLAB with photon energy of 100.5 keV. The lattice parameters $a=5.6963$, $b=2.8497$, and $c=12.417$ Å of the orthorhombic structure at low temperature were verified. This confirms the high crystalline perfection and the absence of impurity phases. The crystal is found to be microscopi-

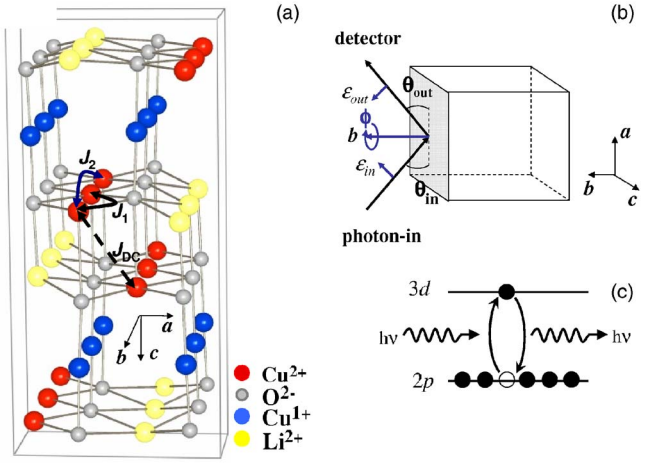

FIG. 1. (Color online) (a) The crystal structure of $LiCu_2O_2$ and the double chains showing J_1, J_2, and J_{DC}. (b) The scattering geometry with photon polarization ε. The azimuthal angle ϕ is 0° in the geometry shown, where the photon polarization is perpendicular to the c axis. (c) An illustration of Cu $2p\rightarrow 3d$ resonant scattering process.

a)Electronic mail: phyandri@nus.edu.sg. Current address: Department of Physics, Faculty of Science, National University of Singapore, 117542 Singapore.

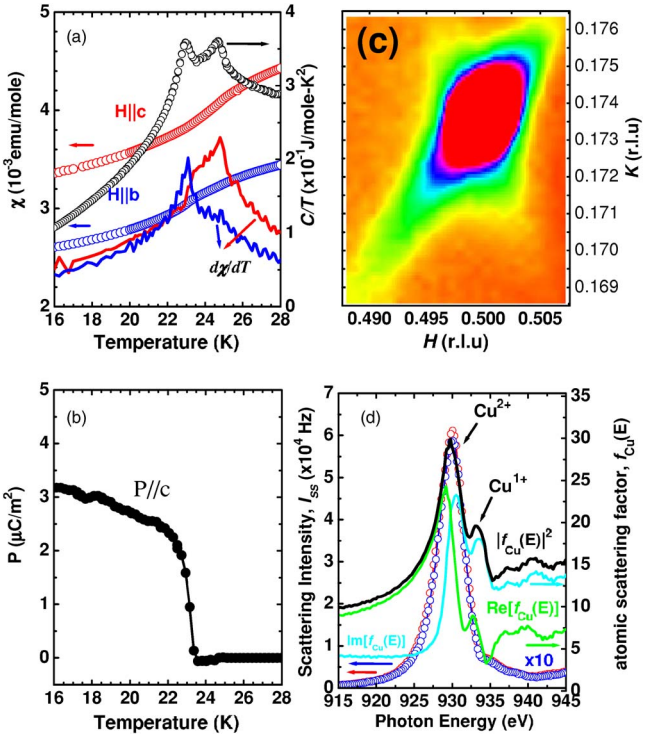

FIG. 2. (Color online) (a) Magnetic susceptibility and heat capacity showing two magnetic transitions, at 23.2 and 24.6 K. (b) The electrical polarization changes along the c axis with the onset of polarization at 23.2 K. (c) The magnetic structure at $E=930$ eV in the reciprocal space map around $(0.5,0.174,0)$ taken at 18 K. The correlation length along the n direction ξ_n is defined as $n_n/\Delta q_n$, where Δq_n is the width of the Bragg reflection and n_n is the lattice parameter along the n direction. (d) Energy scan at fixed $Q=(0.5,\delta,0)$ for two different temperatures: 18 K at $\delta=0.1738$ (red dots) and 24.6 K at $\delta=0.1722$ (blue dots) showing the same profile which indicates the lack of lattice distortion in the FE phase ($T_{FE}=23.2$ K) The result is compared to the complex atomic scattering factor of Cu $f_{Cu}(E)$ to highlight the resonant Cu^{2+} peak.

cally twinned along the [1,1,0] plane with $a\sim 2b$. Below 23 K (T_{FE}), $LiCu_2O_2$ becomes ferroelectric (FE) and shows a small anomaly in the dielectric constant ε.[6] Figure 2(b) shows a changing dielectric polarization (P) along the c direction as a function of temperature. However, the observed polarization ($\sim 4\ \mu C/m^2$) is two to three orders of magnitude smaller compared to $RMnO_3$[8,9] and RMn_2O_5.[9,10]

Two magnetic transitions are found in the magnetic susceptibility χ [Fig. 2(a)]. For an applied magnetic field H parallel to the c axis ($H\|c$), $d\chi_c/dT$ shows two transitions at 23.2 (T_2) and 24.6 K (T_1), while for $H\|b$, the $d\chi_c/dT$ shows only one sharp transition at 23 K. The T_2 coincides with T_{FE} from heat capacity measurements [Fig. 2(a)]. Our sample does not show any other transition below 23 K.[11]

RSXMS was done on a surface which was cleaved *in situ* with (2,1,0) orientation at the beamline X1B of the NSLS using a ten-axis, ultrahigh-vacuum-compatible diffractometer.[12,13] X-ray absorption spectra (XAS) were measured *in situ* in the fluorescence yield mode. We denote the reciprocal space with Miller indices (H,K,L), which represent a momentum transfer $Q=(2\pi H/a, 2\pi K/b, 2\pi L/c)$. The angles of incoming photons (θ_{in}) and outgoing photons (θ_{out}) depend on Q but was approximately 35° and 55°, respectively. The azimuthal angle, ϕ, is $\phi=0°$ and 90° [Fig. 1(b)].

Scattering at transition metal L edges is sensitive to the spin modulation.[14–16] Figure 1(c) illustrates Cu $2p\rightarrow 3d$ resonant scattering process, which enhances the magnetic scattering from Cu^{2+}. In the cuprate systems, the transition exhibits two main peaks corresponding to final states with $2p_{3/2}$ and $2p_{1/2}$ core holes, referred to as the Cu L_3 and Cu L_2 absorption edges, respectively. This material is particularly interesting because it has a clear contrast in the scattering of the Cu^{1+} and Cu^{2+} sites [Fig. 2(d)]. The peaks at 930 and 933 eV are Cu L_3 edge of Cu^{2+} and of Cu^{1+}, respectively.[17]

Probing with resonance photon energy $E=930$ eV, an IC superstructure with $Q=(0.5,0.1738,0)$ at $T=18$ K is observed [Fig. 2(c)]. This is identical to the magnetic superstructure found by neutron diffraction.[5] Our experiment reveals that the correlation lengths along the a, b, and c are very large with $\xi_a=(1662\pm 20)$, $\xi_b=(2120\pm 20)$, and $\xi_c=(935\pm 20)$ Å, respectively. X-rays at 930 eV have a penetration depth of 2500 Å.

Figure 2(d) shows the scattering intensity of the superstructure as a function of photon energy $I_{SS}(E)$, i.e. the resonance profile (RP), at 18 and 24.6 K a. The 24.6 and 18 K measurements represent magnetic scatterings at above and below the FE transition, respectively. The RP is compared to the complex atomic scattering factor $f_{Cu}(E)$. In this case, $I_{SS}\propto|f_{Cu}|^2=|\mathrm{Re}[f_{Cu}]+\mathrm{Im}[f_{Cu}]|^2$. The $\mathrm{Im}[f_{Cu}(E)]$ is determined from the absorptive part of the refractive index $\mathrm{Im}[n]$, which is linearly related to the XAS spectrum, through the relation $\mathrm{Im}[n(E)]=-(r_e\lambda^2N/2\pi V_{cell})\ \mathrm{Im}[\Sigma_i f_i(E)]$, while the $\mathrm{Re}[f_{Cu}(E)]$ is calculated from $\mathrm{Im}[f_{Cu}(E)]$ by performing a Kramers-Kronig transform. Here, r_e is the classical electron radius, λ is the x-ray wavelength, N is the number of Cu in the unit cell, and f_i is the complex atomic scattering factor. The XAS measurement was done with an incident x-ray polarization in the ab plane, at room temperature, corrected for self-absorption, and placed on an absolute scale.[18] A gigantic enhancement occurs in the magnetic-FE state. A lattice distortion would result in orders of magnitude smaller scattering intensities.[12]

We have performed a HXD study to rule out a lattice modulation.[19] Even at 4 K, neither a $(0.5,k\pm\delta,0)$ nor a $(0.5,k\pm 2\delta,0)$ reflection was found supporting that the lattice distortion is extremely small. This is in contrast to ferroelectrics $TbMnO_3$ in which lattice distortions are observed.[20]

Figures 3(a) and 3(b) display the intensity together with the position of the Bragg peak as a function of temperature and polarization of the incoming photon. For $\phi=0°$, we have found the presence of two magnetic transitions: at ~23.2 and ~24.6 K, which is consistent with magnetic susceptibility. The intensity increases as temperature decreases, indicating an enhanced magnetic order upon cooling, while Q also changes with temperature. For $\phi=90°$, the superstructure vanishes rapidly above T_2.

The combination of RSXMS, HXD, magnetic susceptibility, and the electrical polarization measurements provides crucial information regarding the coexistence of FE and magnetic states. At $T_2<T<T_1$, we find: First, $d\chi/dT$ shows an anomaly at T_1 for $H\|c$, implying that the c-direction is an *easy* axis [Fig. 2(a)]; Second, there is no FE, i.e., $P=0$ [Fig. 2(b)]; Third, for $\phi=0°$, RSXMS experiment shows a magnetic Bragg reflection, while for $\phi=90°$, the superstructures are very weak. For spins which have a component of the magnetic moment along the c axis, the polarization factor of the magnetic scattering is $f_{mag}=(\mathbf{e}_{in}\times\mathbf{e}_{out})\cdot\hat{\mathbf{M}}\neq 0$. This im-

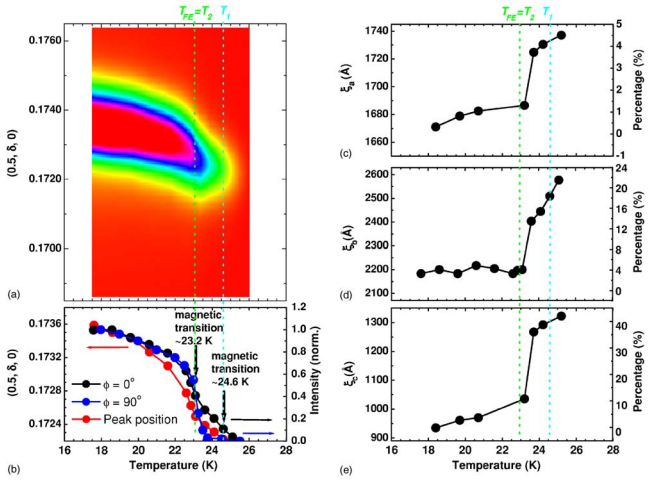

FIG. 3. (Color online) (a) Two-dimensional plot of temperature vs $(0.5, \delta, 0)$ for $\phi=90°$. (b) The evolution of the peak position (red dots), δ, and intensity (black and blue dots) of the magnetic scattering for the two polarizations as a function of temperature showing two transitions: ~23.2 and ~24.6 K. [(c)–(e)] Correlation lengths of the magnetic ordering as function of temperature.

plies that the spins have a strong component or are oriented along the c axis; Fourth, no harmonic and no lattice distortion were found at $Q=2\delta$. A helical structure in ac-plane would result in polarization independence. Therefore, the spin structure is a sinusoidal with the spin oriented along the c axis and propagating with Q along the b direction.

For $T<T_2$ we find the following: First, $d\chi/dT$ shows the magnetic transitions for $H\|b$ and $H\|c$, implying that the b and c are both the easy axes [Fig. 2(b)]; Second, FE is present with $P_c\approx 3\ \mu C/m^2$ [Fig. 3(a)]; Third, f_{mag} is nonzero for both polarizations, $\phi=0°$ and 90°, giving rise to a magnetic Bragg reflection; Fourth, no harmonics and no lattice distortion are found at $Q=2\delta$. These results cannot be explained with a simple spiral spin structure in the bc-plane as such a condition would result in $f_{mag}=0$ for $\phi=90°$. A pure helical or sinusoidal spin wave cannot cause ferroelectricity since $\boldsymbol{P}\cdot\nabla\boldsymbol{M}$ is zero.[21] Therefore, our results are consistent with a spin structure that is helicoidal, having a, b, and c components, and propagating with Q along the b direction. The complexity of the helicoidal structure relates to a coupling of the two frustrated quasi-1D $S=1/2$ chains along the b axis, as shown in Fig. 1(a), resulting to a total polarization P along the c axis. This highlights the underlying frustration which can be lifted by breaking the symmetry yielding an electronically driven ferroelectric order.

Moreover, we find a decreased correlation length in the FE state with decreasing temperature [see Figs. 3(c)–3(e)]. A dramatic change of the coherence lengths occurs around T_2 which is the transition from sinusoidal to helicoidal spin structures. The strongest change is ~42% along c, followed by ~22% along b, and ~4% along the a directions. The strongest distortion is along the c direction, which is also the direction of the ferroelectric moment. This is a surprising result as it cannot be explained by enhanced thermal fluctuations. Usually, the correlation lengths are getting shorter at high temperatures, FE domains form below T_2 in the helicoidal spin phase disturbing the magnetic coherence lengths while the sinusoidal spin structure above T_2 is free of FE domains. This increases the coherence length above T_2.

Another interesting observation is the smallness of the temperature *window* between the two transitions. In $TbMnO_3$,[19] the temperature window is ~12 K. In $CoCr_2O_4$,[22] the temperature window is ~65 K. This supports our picture of an electronically driven phase. Related to this is an increased coherence length with increasing temperature above T_{FE} indicating remaining dynamic FE domain ordering.

In conclusion, we have found two magnetic transitions in $LiCu_2O_2$: a sinusoidal spin structure at $T_2<T<T_1$ and a helicoidal spin structure at $T<T_2$, giving rise to ferroelectricity. The coherence lengths of the superstructure behave in an unusual way, i.e., increasing as the temperature increases. Our results highlight the value of RSXMS for studying the interplay of spin, charge, and lattice degrees of freedom in multiferroics.

We acknowledge M. Mostovoy for helpful discussions and financial support by the Helmholtz Association VH-FZ-007, DFG Ru 773/2-3, DE-FG02-06ER46285, NSLS No. DE-AC02-98CH10886, the Canadian funding agencies: NSERC, CIAR, and CFI, NSF-MDR-0405682.

[1] R. A. Erickson, Phys. Rev. **85**, 745 (1952); A. Yoshimori, J. Phys. Soc. Jpn. **14**, 807 (1959).
[2] S.-L. Drechsler, J. Málek, J. Richter, A. S. Moskvin, A. A. Gippius, and H. Rosner, Phys. Rev. Lett. **94**, 039705 (2005).
[3] L. Capogna, M. Mayr, P. Horsch, M. Raichle, R. K. Kremer, M. Sofin, A. Maljuk, M. Jansen, and B. Keimer, Phys. Rev. B **71**, 140402(R) (2005).
[4] S. Zvyagin, G. Cao, Y. Xin, S. McCall, T. Caldwell, W. Moulton, L.-C. Brunel, A. Angerhofer, and J. E. Crow, Phys. Rev. B **66**, 064424 (2002).
[5] T. Masuda, A. Zheludev, A. Bush, M. Markina, and A. Vasiliev, Phys. Rev. Lett. **92**, 177201 (2004).
[6] S. Park, Y. J. Choi, C. L. Zhang, and S.-W. Cheong, Phys. Rev. Lett. **98**, 057601 (2007).
[7] A. A. Gippius, E. N. Morozova, A. S. Moskvin, A. V. Zalessky, A. A. Bush, M. Baenitz, H. Rosner, and S.-L. Drechsler, Phys. Rev. B **70**, 020406(R) (2004).
[8] T. Kimura, G. Lawes, T. Goto, Y. Tokura, and A. P. Ramirez, Phys. Rev. B **71**, 224425 (2005).
[9] S.-W. Cheong and M. Mostovoy, Nat. Mater. **6**, 13 (2007).
[10] N. Hur, S. Park, P. A. Sharma, J. S. Ahn, S. Guha, and S.-W. Cheong, Nature (London) **429**, 392 (2004).
[11] E. M. L. Chung, G. J. McIntyre, D. McK. Paul, G. Balakrishnan, and M. R. Lees, Phys. Rev. B **68**, 144410 (2003).
[12] P. Abbamonte, L. Venema, A. Rusydi, G. A. Sawatzky, G. Logvenov, and I. Bozovic, Science **297**, 581 (2002).
[13] A. Rusydi, P. Abbamonte, H. Eisaki, Y. Fujimaki, S. Smadici, N. Motoyama, S. Uchida, Y.-K. Kim, M. Rübhausen, and G. A. Sawatzky, Phys. Rev. Lett. **100**, 036403 (20008).
[14] C. Kao, J. B. Hastings, E. D. Johnson, D. P. Siddons, G. C. Smith, and G. A. Prinz, Phys. Rev. Lett. **65**, 373 (1990).
[15] K. J. Thomas, J. P. Hill, S. Grenier, Y.-J. Kim, P. Abbamonte, L. Venema, A. Rusydi, Y. Tomioka, Y. Tokura, D. F. McMorrow, G. Sawatzky, and M. van Veenendaal, Phys. Rev. Lett. **92**, 237204 (2004).
[16] C. Schüßler-Langeheine, J. Schlappa, A. Tanaka, Z. Hu, C. F. Chang, E. Schierle, M. Benomar, H. Ott, E. Weschke, G. Kaindl, O. Friedt, G. A. Sawatzky, H.-J. Lin, C. T. Chen, M. Braden, and L. H. Tjeng, Phys. Rev. Lett. **95**, 156402 (2005).
[17] L. H. Tjeng, C. T. Chen, and S.-W. Cheong, Phys. Rev. B **45**, 8205 (1992).
[18] B. L. Henke, E. M. Gullikson, and J. C. Davis, At. Data Nucl. Data Tables **54**, 181 (1993).
[19] T. Kimura, T. Goto, H. Shintani, K. Ishizaka, T. Arima, and Y. Tokura, Nature (London) **426**, 55 (2003).
[20] N. Aliouane, D. N. Argyriou, J. Strempfer, I. Zegkinoglou, S. Landsgesell, and M. v. Zimmermann, Phys. Rev. B **73**, 020102(R) (2006).
[21] M. Mostovoy, Phys. Rev. Lett. **96**, 067601 (2006).
[22] Y. Yamasaki, S. Miyasaka, Y. Kaneko, J.-P. He, T. Arima, and Y. Tokura, Phys. Rev. Lett. **96**, 207204 (2006).